26th EPS Conf. on Contr. Fusion and Plasma Physics, Maastricht, 14 - 18 June 1999 ECA Vol.23J (1999) 1325 - 1328

Ablation and Acceleration of Impurity Pellets Interacted with Fast Ions of NBI in CHS Heliotron/Torsatron

Y. Shirai[1)], S. Morita, M. Goto, M. Isobe, X. Gong[2)], K. Matsuoka, H. Nihei[3)], T. Minami, S. Nishimura, Y. Ogawa[3)], S. Okamura, M. Osakabe, S. Takagi[4)], C. Takahashi, K. Tanaka, K. Toi, B. Wan[2)], Y. Yoshimura

National Institute for Fusion Science, Toki 509-5292, Japan
1) The Graduate University for Advanced Studies, Toki 509-5292, Japan
2) Institute of Plasma Physics, Academia Sinica, 230031, Hefei, Anhui, China
3) Univ. of Tokyo, Hongo, Bunkyo-ku, Tokyo113-8656, Japan
4) Department of Energy Engineering Science, Nagoya Univ., Nagoya 464-0814, Japan

1. Introduction

The impurity pellet injection into the fusion plasma has been studied as a powerful tool for the diagnostic application [1-3]. The understanding of the mechanism for the ablation is especially important since the feasibility of the diagnostic application depends on the ablation process of the impurity pellet interacted with the hot plasma. We have carried out impurity pellet injection experiments on Compact Helical System (CHS) for the ablation study. A preliminary report has been made on the study of the plasma response after impurity pellet injection in CHS [4]. In this paper, some results of the ablation characteristic on the impurity pellet injection experiments in the NBI and ECH plasmas of CHS are described. In order to clarify the impurity pellet ablation, two CCD cameras and an eleven optical fiber array were employed to observe the three-dimensional pellet trajectory and the local ablation in detail.

2. Experimental set-up

CHS is a heliotron/torsatron type device (magnetic axis R_{ax}=0.88~1.01m, averaged minor radius a=0.17~0.21m, toroidal magnetic field $B_t \leq 2$T) with l=2 and m=8 [5]. In this experiment, B_t is fixed at 0.9T, and R_{ax} is set at 0.92m and 0.99m for the ECH and NBI plasmas, respectively. In CHS two neutral beam lines, NBI#1 and NBI#2 are installed. Both of them are injected tangentially and are balanced each other to cancel out the beam-driven current. The pellets used in this experiment are spheres of hydrocarbon (di-vinyl-benzene polystyrene) with a diameter of 0.3mm. The spherical pellet is accelerated by a pressurized helium gas. A velocity of the pellet is 270 m/s in this experiment. The pellet velocity is measured by time-of-fight method which consists of a photo-diode and a diode laser. Two CCD camera systems with an interference filter of CI (λ_0=538nm, FWHM=2nm), which were installed on top ('top CCD camera') and outboard side ('outside CCD camera') ports near the pellet injector,

respectively. The pellet trajectory is simultaneously photographed by these CCD cameras from two directions. An eleven-channel optical fiber array with an interference filter of CI was installed on the opposite side (inboard side) port of the pellet injector (ch1~ch11 in Fig. 1(a)). In order to observe the local pellet ablation, the radial viewing angle is narrowed by a vertical slit mounted in front of the fibers. In the case of R_{ax}=0.921m, the radial spatial resolution along the pellet path is 19mm and the toroidal spatial resolution is 142mm, and in the case of R_{ax}=0.995m, 23mm and 176mm. The total time evolution of the pellet ablation is observed by a wide-angle optical fiber with an interference filter of CI from the backside of the injector.

3. Experimental results

A typical experimental result on the pellet injection into the ECH plasma (P_{ECH}= 200kW, f_{ECH}=53GHz,) is shown in Fig. 1. The central electron temperature and the line-averaged density are $T_e(0)$=1keV ($T_i(0)$~200eV) and $\bar{n}_e=1\times10^{19}m^{-3}$. Figures 1 (a) and (b) show photographs taken from the top and outside CCD cameras. Thick lines in Fig. 1 (a) indicate the viewing angle of the outside CCD camera. The path of the pellet injection is offset from the normal to the magnetic field line by 29° in the toroidal direction. Signals from the eleven-channel fiber array and the wide-angle fiber are shown in Fig. 1(c). As the pellet moves toward the plasma center, the ablation becomes stronger. It is seen that the pellet penetrates straightly in the ECH plasma, and is completely ablated at ρ=0.4. The peak of the ablation can be estimated to be ρ=0.4~0.5. Here, the size of the ablation cloud is 14±1mm and 20±4mm in the toroidal and poloidal directions, respectively.

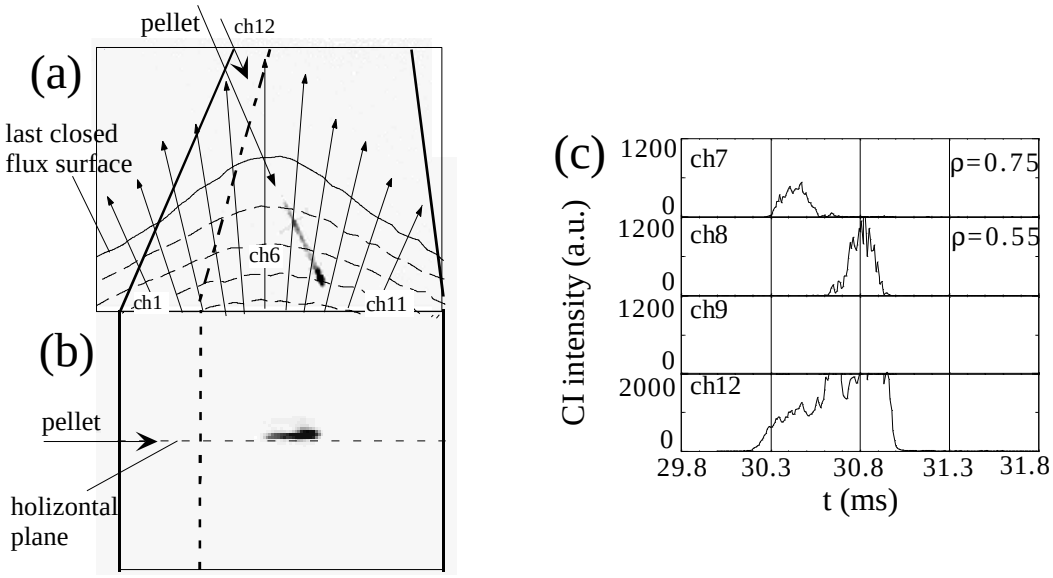

Fig. 1 Photographs of top(a) and outboad side(b) CCD cameras and signals from optical fiber array(ch7~ch9) and wide-angle optical fiber(ch12)(c) with hydrocarbon pelletinjection in ECH plasma.

Experimental results on the pellet injection in the NBI#1 co-injection plasma (P_{NBI}=900kW, E_{NBI}=40keV) are shown in Fig. 2. In this experiment, we adjusted the same electron density ($\bar{n}_e=1\times10^{19}m^{-3}$) as the ECH case, although the temperature is much low ($T_e(0)=T_i(0)$=200eV). A completely different result was obtained in this experiment compared with the case of ECH. Figures (a) and (b) are photographs taken from the top and outside CCD cameras. The directions of the fast ions of the NBI and the toroidal magnetic field (B_t) are shown in Fig. 2(a). The drastic deflection of the pellet trajectory can be seen in the toroidal and poloidal directions. Signals from the fiber array and the wide-angle fiber are shown in Fig. 2(c). In contrast with the ECH result, it is understood that the pellet is strongly ablated at the plasma outer region (ρ~0.7). As the pellet moves to the plasma center, the ablation becomes weaker. The peak of the ablation estimated to be ρ~0.7. Th size of the ablation cloud is 9±1mm and 20±2mm in the toroidal and radial directions, respectively, and these values are nearly the same as the ECH case. Furthermore, the pellet velocity is also measured from the two CCD cameras and the fiber array. We found for the first time that the pellet is accelerated from 270m/s at the plasma edge to 700m/s near the plasma center (see Fig. 3), although the pellet velocity is constant in the ECH plasma. In order to confirm that these phenomena really originate in the effect of the fast ions of NBI, the further pellet injection was carried out using the NBI#2 co-injection plasma. It should be noticed that the toroidal direction of the NBI#2 is opposite to the NBI#1 case. Experimental results are shown in Fig. 4. The deflection of the pellet trajectory is also seen in the toroidal and poloidal directions. The direction of the pellet deflection is clearly

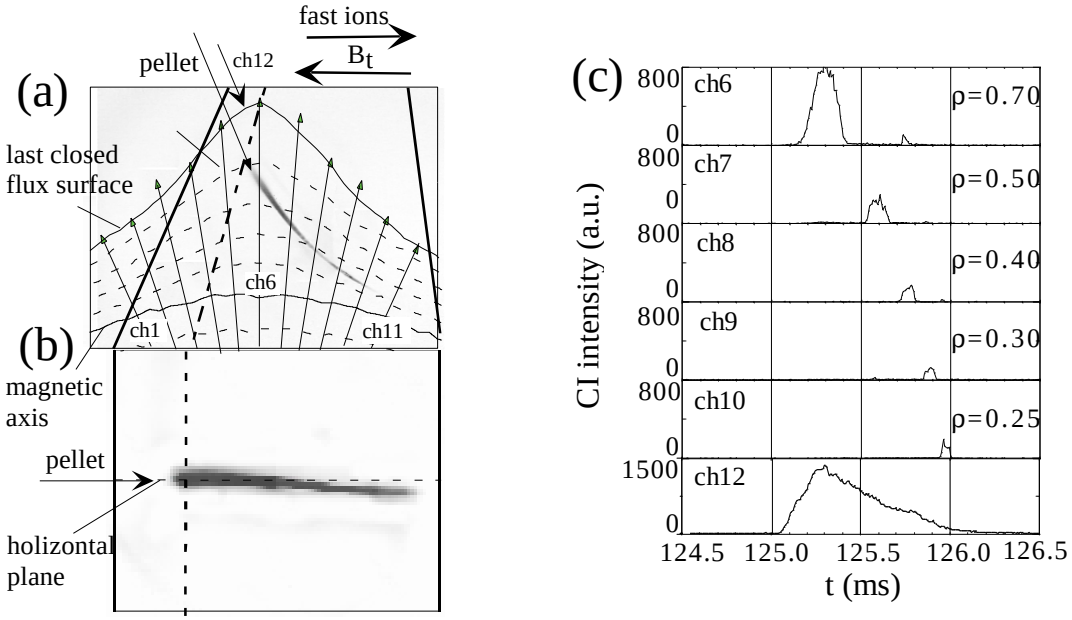

Fig. 2 Photographs of top(a) and outboad side(b) CCD cameras and signals from optical fiber array(ch6~ch10) and wide-angle optical fiber(ch12)(c) with hydrocarbon pellet injection in NBI#1 plasma.

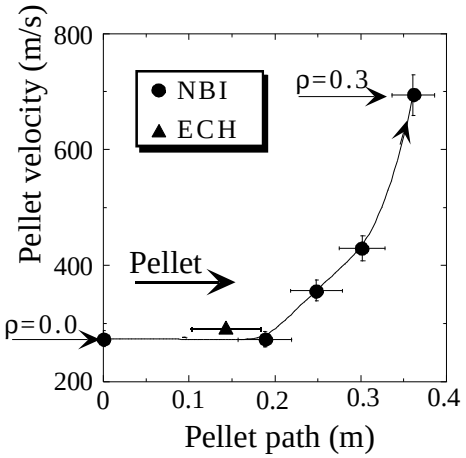

Fig. 3 Spatial distribution of pellet velocity

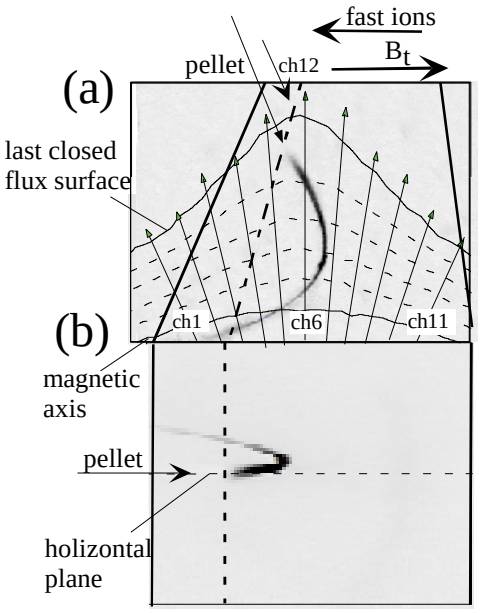

Fig. 4 Photographs of top(a) and outboad side(b) CCD cameras with hydrocarbon pellet injection in NBI#2 co-injection plasma.

inverted and coincides with the direction of the fast ions of the NBI.

4. Summary

The hydrocarbon pellet injections have been carried out in the ECH and NBI plasmas on CHS for the ablation study. As a result, it is found that the pellet is strongly ablated at the plasma edge and is deflected due to the impact of the fast ions from the NBI, although the pellet moves straightly in the ECH case. Furthermore, we found for the firs time that the pellet velocity is accelerated from 270m/s at the plasma edge to 700m/s near the plasma center. These results clearly demonstrate that the interaction with fast ions is an essential mechanism for the pellet ablation in the NBI plasma of helical devices.

Reference

[1] R.K.Fisher, et al., Fusion Technol. **13**, 536 (1988).

[2] E.S.Marmar, et al., Rev. Sci. Instrum. **60**, 3739 (1989).

[3] S. Morita, et al., Nucl. Fusion **30**, 938 (1990).

[4] Y. Shirai, et al., J. of Plasma and Fusion Research SERIES, Vol. 1, 302 (1998).

[5] K. Matsuoka et al., in Plasma Physics and Controlled Nuclear Fusion Research, Vol. 2, 411 (1988).